Int J Fatigue **11** No 3 (1989) pp 177–182

Cyclic properties of coarse-grained cast austenitic manganese steels

D. Rittel and I. Roman

The cyclic properties of coarse-grained cast austenitic manganese (Hadfield) steels were studied. The material cyclically hardens, with a pronounced memory effect which is common to austenitic steels. The cyclic flow curves were different for the wrought and the cast condition of the material; however low cycle fatigue properties are similar for the two conditions. Typical features of monotonic deformation and fracture (*ie* orange peel and surface coarse slip bands) were also noted on the surface of compact tension specimens used for fatigue crack growth rate measurements. Contrary to the monotonic case, these deformation features do not markedly affect the cyclic cracking process.

Keywords: austenitic manganese steel; intermittent overload; low cycle fatigue

Cast austenitic manganese (Hadfield) steels have long been known for their outstanding wear and toughness properties, and these subjects have been extensively studied.[1] On the other hand, work on the cyclic properties of these steels is less documented. Available research on fatigue properties[2–4] has focussed on hot-rolled Hadfield steel with the main purpose to investigate the effect of intermittent overload peaks and to test different materials for their energy absorption capacities.

In response, this paper reports and discusses basic cyclic properties of coarse-grained cast austenitic manganese steels *per se*, and the results are compared with available data on hot-rolled material. The cyclic properties of this steel are of additional interest since coarse-grained materials in general exhibit characteristic transitional mechanical properties (from single to true polycrystalline), along with the fact that Hadfield steels in particular possess a special combination of strain-hardening and tensile ductility.

Experimental

Materials

Four commercial heats of cast austenitic manganese steel were employed, and their composition and monotonic mechanical properties are listed in Tables 1 and 2, respectively. Heat MS1 is of standard Hadfield composition; small additions of alloying elements were introduced in the other heats. The basic casting procedure, solution heat treatment and resulting microstructure have been reported previously.[5–7] It is worth mentioning that the materials' microstructure is fully austenitic and grain sizes vary from hundreds of microns to one mm. The material is sound and few carbides are discernable. The dendritic pattern does not disappear as a result of the solution heat treatment and can be observed after repeated etching. All the specimens were initially rough machined and final dimensions were obtained by fine grinding to avoid the formation of a hardened surface layer which is characteristic of Hadfield steels.

Table 1. Composition (in wt%) of the investigated heats

Element	C	Mn	Si	P	S	Cr	Ni	Mo	Ti
Heat									
MS1	1.25	13.1	0.47	0.030	0.008	0.13	0.1	–	–
MS4A	1.06	13.4	0.87	0.051	0.003	1.30	–	0.66	0.14
MS4B	1.11	12.6	0.71	0.047	0.01	1.11	0.26	0.89	0.04
MS4C	1.13	12.5	0.55	0.028	0.01	1.14	0.24	0.59	0.06

Cyclic mechanical properties

Round low cycle fatigue (push–pull) specimens, 6.25 mm in diameter, were employed for the determination of cyclic mechanical properties. A longitudinal clip gauge was used for the determination of the applied longitudinal strain. Testing was performed on a closed loop servo-hydraulic tensile machine (MTS 810), and specimen alignment was ensured by utilizing a Wood's metal grip. The cyclic mechanical

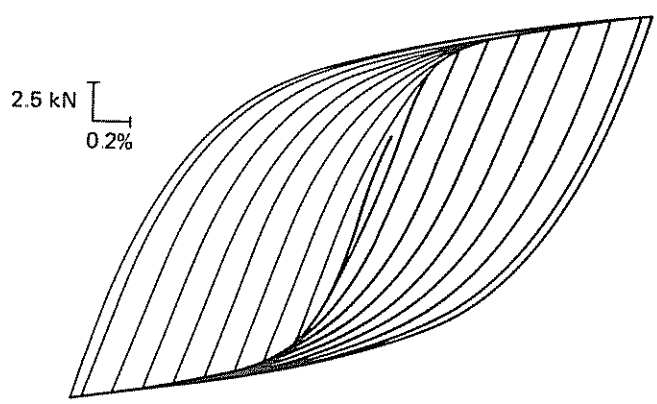

Fig. 1 Typical strain control mechanical hysteresis loops (load *vs* strain)

properties were determined from a single specimen after stabilization, employing the block method followed by pulling to fracture as recommended.[8] Testing was carried out at room temperature in air.

Strain *versus* cycles to failure

Sustained strain *versus* number of cycles to fracture was determined employing the push–pull specimen described. Testing frequency was 20Hz.

Crack growth rate

Precracked compact tension specimens (30 mm width) were utilized for fatigue crack growth rate determination. According to ASTM E647–83 requirements regarding specimen dimensions,[9] the effective strength was taken as the mid-value between yield and true fracture strength of the material, *ie* 875 MPa. The true fracture strength was employed instead of the ultimate tensile strength, since Hadfield steels fracture without necking.[1,6,7] Crack advance was monitored with a travelling optical microscope and data reduction to da/dN *versus* ΔK was done according to recommended procedure.[9]

Results and discussion

Cyclic mechanical properties

Typical strain-control mechanical hysteresis loops, shown in Fig. 1, were recorded during initial cycling of the specimens. These loops are indicative of cyclic hardening behaviour of the cast material, similar to previous observations for the wrought condition.[2,4] Therefore, the rule of thumb which predicts cyclic hardening or softening on the basis of the static mechanical properties is obeyed too.[10] The cyclic 0.2% yield strength of the various heats is given in Table 3, along with the stabilization strain and the ratio of the cyclic to monotonic yield strength. Despite stabilization, a strong dependence of the cyclic strength upon stabilization strain exists, and they both increase concurrently. Therefore, cyclic yield strength cannot be specified as a material property as it depends on the previous mechanical history. This fact was not noted previously for Hadfield steels, whereas a similar memory effect has been reported in studies of austenitic stainless steel.[11,12] Moreover, it has been established that a unique cyclic stress–strain curve is characteristic only of materials exhibiting wavy slip,[13] and that those do not include Hadfield or austenitic stainless steels. It therefore seems that,

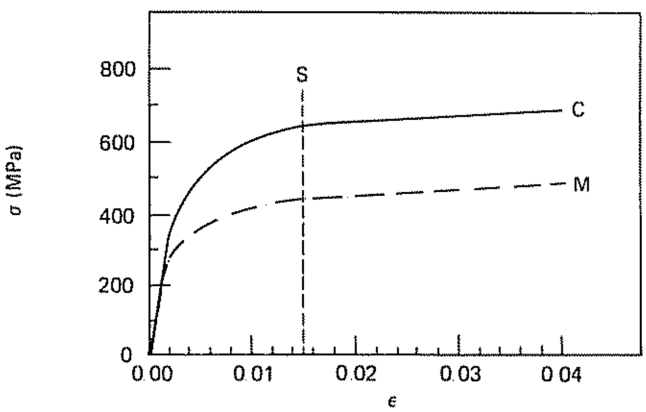

Fig. 2 Typical cyclic (C) and monotonic (M) stress–strain curves (S indicates stabilization strain)

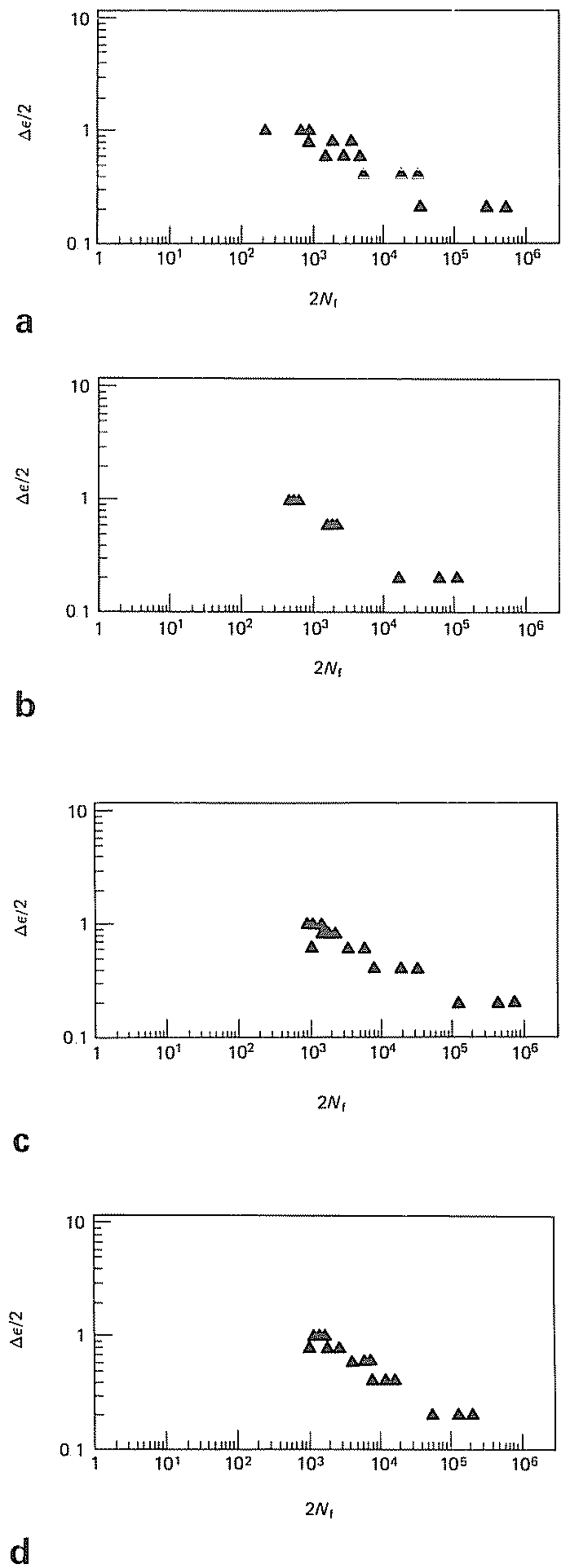

Fig. 3 Typical strain–life curves for the four investigated heats: (a) MS1; (b) MS4A; (C) MS4B; and (d) MS4C

in general, austenitic steels cannot be characterized by a unique cyclic stress–strain curve. This situation imposes limitations on the applicability of the single specimen technique. In addition, bearing in mind that plastic deformation is a path dependent process, it is recommended that stabilization strain be mentioned when reporting cyclic mechanical properties.

The cyclic (C) and monotonic (M) stress–strain behaviour of Hadfield steels are shown in Fig. 2. The two curves are parallel even past the stabilization strain (S), indicating identical strain-hardening behaviour. It is assumed that the stress–strain relationship is described by the sum of a constant stress (Peierls stress) and a structure dependent term (via Burgers vector), in which case the experimental results indicate that the structure dependent term in unaffected by cycling. Cyclic hardening or softening is associated with changes occurring in the dislocation sub-structure of the material. Low stacking fault energy (SFE) materials develop planar arrays of dislocations upon cycling[12] whereas high SFE materials exhibit dislocation cells.[13] Since Hadfield steels possess a low SFE,[14] the present results suggest that planar dislocation arrays do not markedly affect the cyclic strain-hardening properties of the cast material as the structure is not effectively refined by cell formation. It should be emphasized that the present results contradict previous reports on wrought Hadfield steels,[3,4] where the cyclic and monotonic flow curves were not parallel. The reason for this difference is not clear; apart from the fact that the investigated material was hot rolled and of a much finer grain size when compared with the present coarse-grained cast steel. It seems that both factors make it difficult to compare the cast and wrought conditions from the point of view of cyclic hardening.

Strain–life curves

Strain–life graphs (overall strain, cycles to failure) for the various heats are shown in Fig. 3. The fatigue strength exponent and the fatigue ductility exponent were determined on the basis of Manson's equation for cyclic strains.[8] It was assumed that the values of the fatigue strength coefficient (σ'_f) and of the fatigue ductility (ε'_f) are identical to their monotonic equivalents.[8] The transitional number of reversals to failure (indicating transition from a plastic to elastic strain controlled process) was also determined, and all results are summarized in Table 4. These results indicate that, despite differences in composition and strength, all four experimental heats exhibit nearly identical low cycle fatigue properties. This is in contrast with previous experimental results on the high-cycle fatigue properties which show that the slope

Table 2. Average mechanical properties of the investigated heats

Heat	σ_y, 0.2% (MPa)	σ_{FRAC} (MPa)	Elongation (%)	Reduction of area (%)
MS1	350	1350	38	43
MS4A	430	1230	38	35
MS4B	430	1320	44	40
MS4C	407	1357	54	36

Table 3. Typical cyclic yield strength and ratio of cyclic to monotonic yield strength of Hadfield steels (R). A dependence of the cyclic yield strength on the stabilization strain is noticeable

	1/2ε stabilization (%)	Cyclic σ_y, 0.2% (average) (MPa)	R
MS1	1.50	499	1.36
	1.72	606	1.67
MS4A	0.58	453	1.05
MS4B	1.98	597	1.35
MS4C	1.20	542	1.35
	1.94	640	1.55
	1.98	667	1.64

Table 4. Low cycle fatigue properties of cast Hadfield steels

Heat	Fatigue strength exponent (b)	Fatigue ductility exponent (c)	Transitional reversals to failure ($2N_T$)
MS1	−0.0373	−0.632	846
MS4A	−0.0344	−0.663	588
MS4B	−0.0289	−0.576	1520
MS4C	−0.0321	−0.562	1929

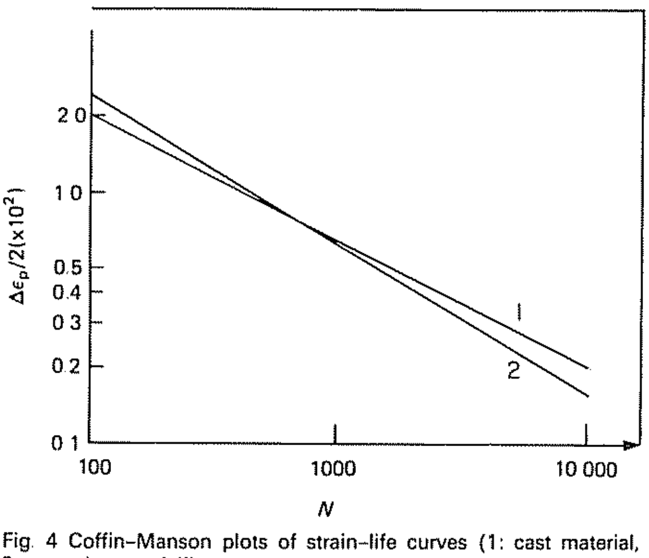

Fig. 4 Coffin–Manson plots of strain-life curves (1: cast material, 2: wrought material[4])

of the transition domain (from finite to infinite life) increases from about 0.50 to 2.20 MPa^{-1} as a result of an increase in phosphorus level of 0.020 to 0.065 wt%.[5]

The former study also suggests that the phosphorus level affects fatigue crack propagation rather more than crack initiation. However, in low cycle fatigue tests, initiation of fatigue cracks dominates the overall fatigue life. Consequently, it is not surprising that low cycle fatigue properties are not affected by the phosphorus level in the investigated range.

To compare wrought and cast material, a Coffin–Manson plot of the plastic strain *versus* cycles to failure was constructed, employing average values of the fatigue ductility exponent, $c = -0.608$ and $\varepsilon'_f = 0.4$ for the cast material. This plot, along with former results for the wrought material,[4] is shown in Fig. 4. The results indicate that cast Hadfield steels do not exhibit inferior properties with respect to the wrought material, and even appear to be superior in the lower strain region. The strain-life properties of Hadfield steels are rather insensitive to structural parameters and thermomechanical treatments, providing soundness of the material is ensured.

Crack growth rate

The reduced fatigue crack growth rate data is plotted as a function of the stress intensity range (Fig. 5). The results show identical behaviour for all investigated heats. According to ASTM standard E647–83, the data is valid if the effective yield strength is used for the present case of a high strain-hardening material. However, despite extensive plasticity at high crack growth rates, the linear relationship between da/dN and ΔK is preserved (on the logarithmic scale). It is therefore proposed that ΔK be considered as a parameter characterizing the applied stresses, rather than as a measure of the cyclic crack-tip singularity in the sense of fracture mechanics.[15]

The macroscopic appearance of the specimens is shown in Fig. 6 for both small scale (up to 30 $MPam^{1/2}$) and general yield conditions. Yielding causes a strong surface alteration of the 'orange-peel' type similar to observations on the tensile deformation of this material.[6] It seems that orange peel formation is a general feature of the material which is experienced regardless of the type of loading. For monotonic loading, surface instabilities and coarse slip bands were related to deformation and fracture mechanisms of Hadfield steels.[6,7] It is therefore important to ascertain the extent to which these features participate in the cyclic fracture process.

The cyclic fracture process

The fracture surface topography of compact tension and push–pull samples was examined using a scanning electron microscope. The typical fracture surface topography of a compact tension specimen is shown in Fig. 7. As a result of the coarse grain-size of the material, individual fractured grains are easily discernible on the fracture surface. The crack front can be identified at various stages of the crack propagation. This front is mildly curved vertically up the page in Fig. 7. This indicates that there is no tendency for increased crack growth in the vicinity of the free surfaces of the specimen. The 'low ΔK' portion (up to about 15 $MPam^{1/2}$) of the fracture surface is characterized by transgranular feather-like morphology. As ΔK increases, well defined striations appear along with extensive secondary cracking. Identical fracture features (*eg* crack arrest lines and striations) were also noticed on the fracture surface of push–pull specimens. The side surfaces of compact tension specimens were examined by light microscopy in the vicinity of the crack tip and along the crack propagation profile (Fig. 8). Surface coarse slip bands dictated the microscopic crack propagation path and the crack tip was found to lie in such a band. Typical micrographs of a polished and etched mid-thickness section (parallel to the side surface) of a compact tension specimen are shown in Fig. 9. Coarse slip bands are still noticeable, but to a lesser extent, and they concentrate along the crack profile and at the tip itself. These observations indicate that coarse slip band development is intensified on the surface of the specimen as a result of the characteristic surface deformation by orange-peel formation. Coarse slip band occurrence during monotonic straining of Hadfield steels has been reported previously and low strain surface cracking initiates within such bands.[6] It is also interesting to note that for high cycle fatigue specimens, coarse slip bands were observed to form in surface grains at stress levels well below the yield strength, and they indicated local micro yielding of the material.[5] In the present case, since there are no indications of increased crack growth near the free surfaces of the specimen, it can be concluded that surface coarse slip bands do not significantly affect the overall rate of crack growth. Rather, their main contribution is the determination of the microscopic crack path. It should be emphasized that this observation applies to the present near plane-strain of deformation, in which the plastic zone size is constant throughout the thickness of the specimen. If deviations from plane-strain deformation occur, surface cracking at low strains is expected to accelerate the overall cracking process as the plastic zone size increases near the free surfaces of the specimen. It can therefore be concluded that characteristic deformation and fracture features which occurred during monotonic and high cycle fatigue loading of Hadfield steels are also operative during low cycle fatigue of this material. However, their contribution to the overall crack growth process is negligible for plane strain cyclically deforming specimens.

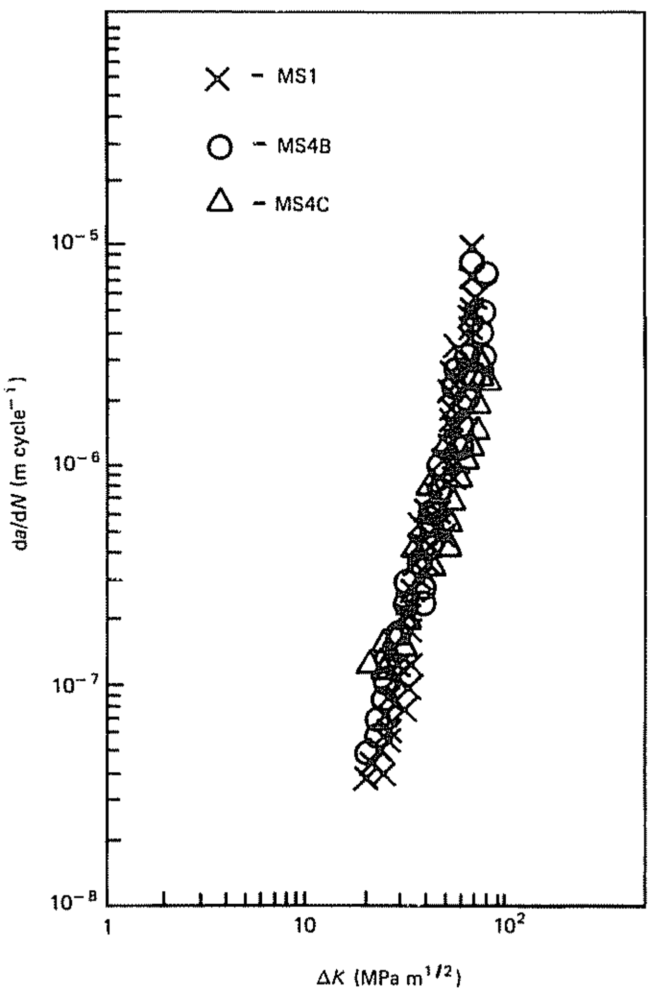

Fig. 5 Reduced crack-growth rate as a function of the stress intensity range

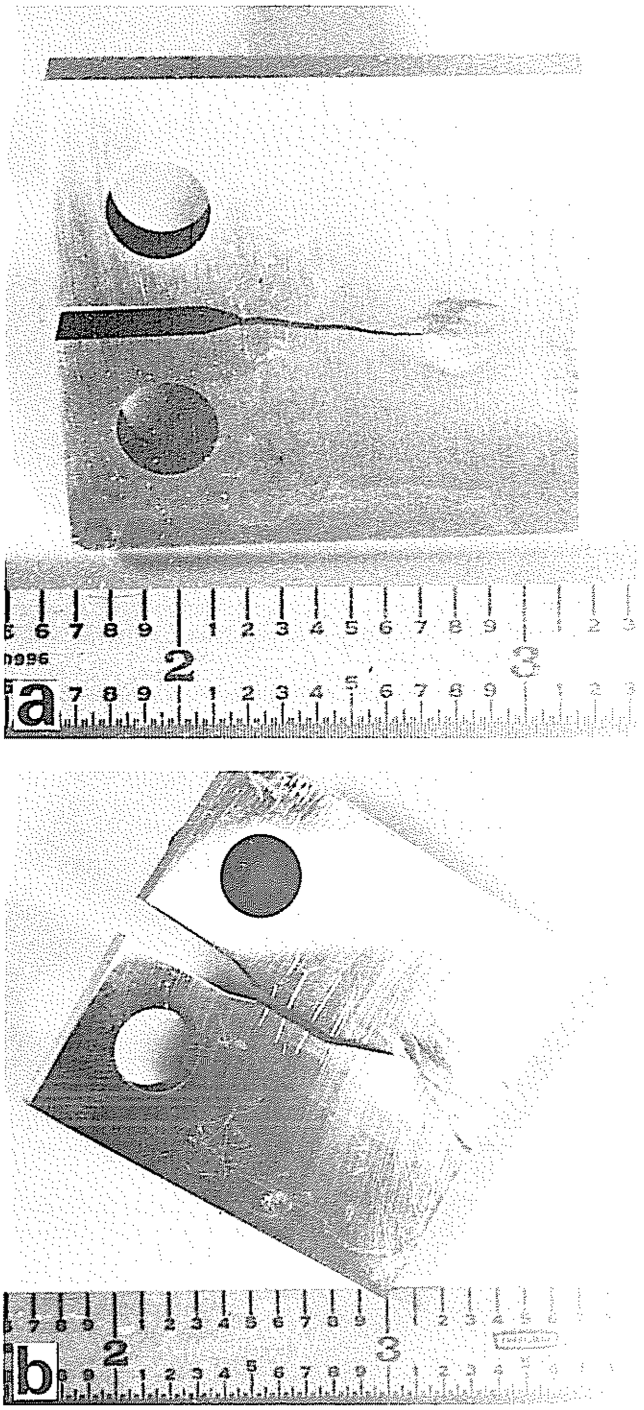

Fig 6 Typical compact tension specimens showing: (a) small scale yielding (ΔK) up to 30 MPam$^{1/2}$); and (b) large scale yielding (ΔK up to 80 MPam$^{1/2}$)

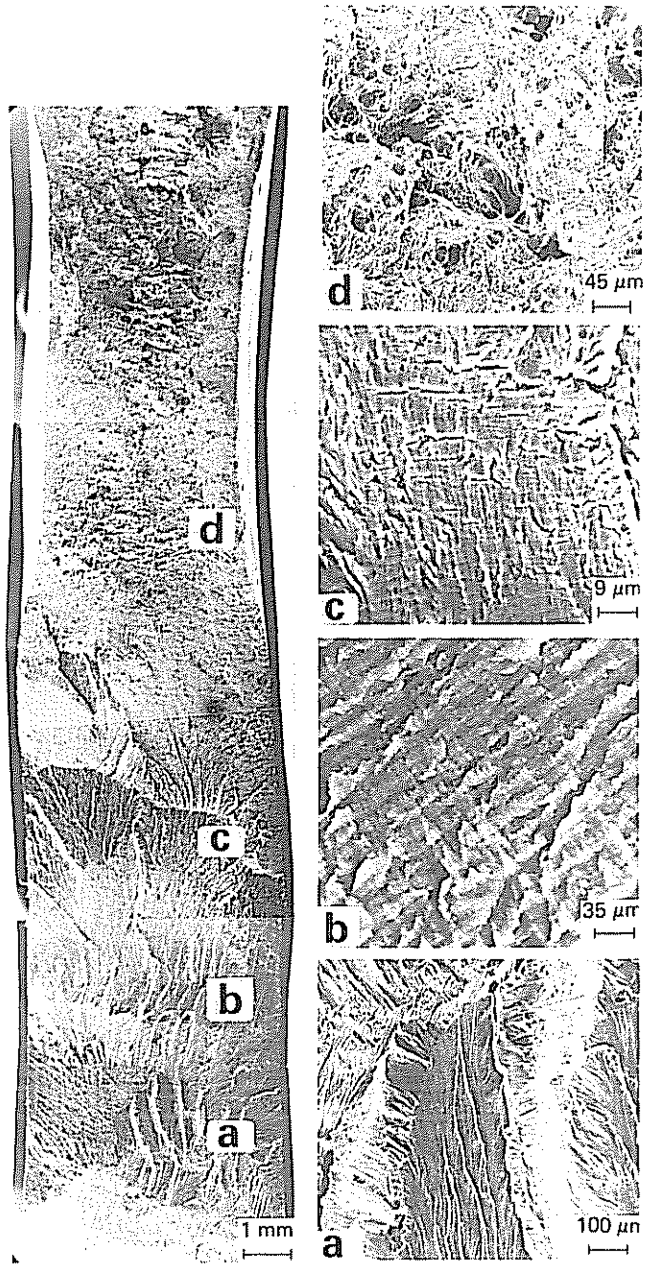

Fig 7 Typical fractographs of a compact tension specimen showing: (a) transgranular featherlike morphology; (b) ill-defined striations; (c) coarse striations and secondary cracking; and (d) Monotonic tensile overload dimples Crack propagation occurred in the direction vertically up the page

Conclusions

Cyclic properties of four different heats of coarse-grained cast austenitic manganese steel have been characterized Despite differences in composition, these heats behave nearly identically in the low cycle fatigue region.

Cast Hadfield steels cyclically harden; however, the degree of hardening depends on the stabilization pre-strain level, and the high stress-hardening capacity of the material is not degraded by cycling.

Characteristic deformation and fracture features (*eg* orange peel and coarse slip bands) observed during monotonic loading are also observed during cyclic loading. However, these features do not significantly accelerate the cracking process for plane-strain deforming specimens

Acknowledgement

The authors would like to express their gratitude to Urdan Associated Steel Foundries (Natanya, Israel) for providing experimental material and samples.

References

1 Metals Handbook *'Austenitic Manganese Steel'* Vol 3 9th Edition (American Society for Metals. 1980) pp 568–588

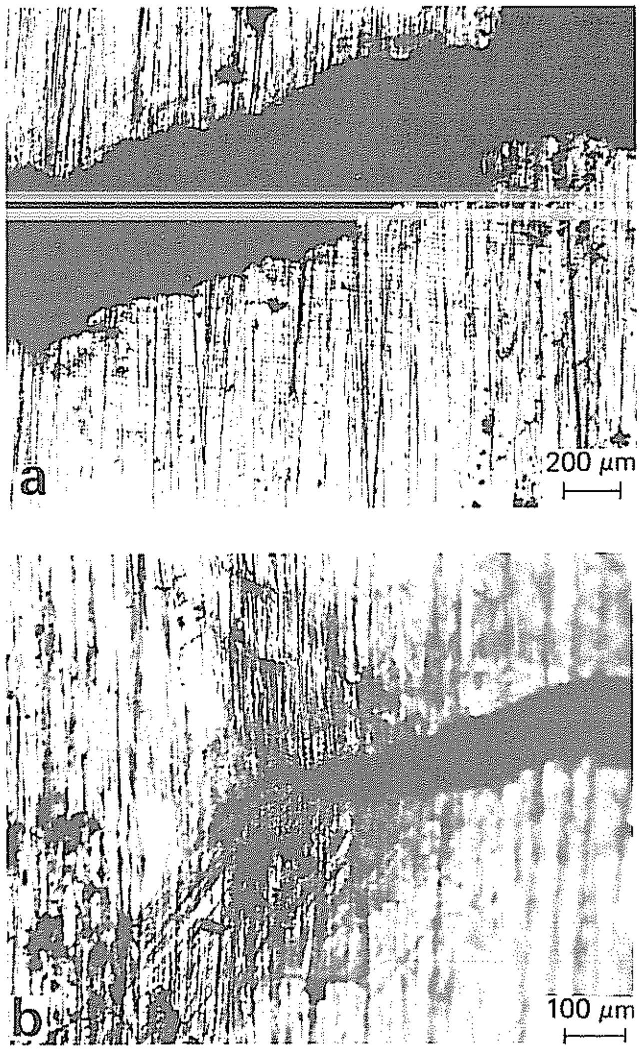

Fig 8 View of the side surface of a compact tension specimen, showing: (a) Coarse slip bands along the path of the crack, perpendicular to the vertical scratches; and (b) Crack-tip laying in coarse slip bands

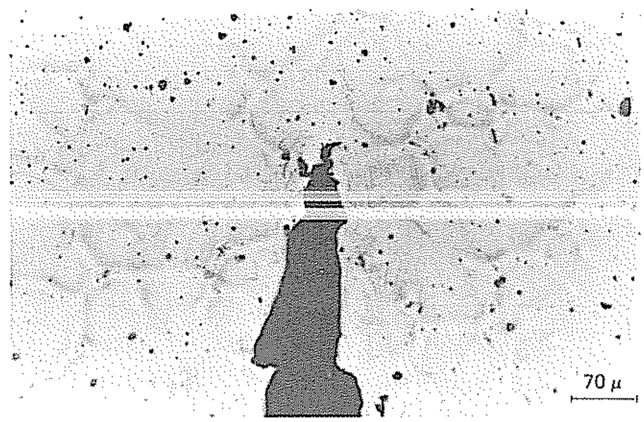

Fig 9 Mid-thickness metallographic section (Nital 3%) of the specimen shown in Figure 8: coarse slip bands in the vicinity of the crack-tip are less discernable

2 **Stephens, R.I., Saxena, C.P. and Rice, R.C.** 'Fracture toughness and subcritical crack growth of austenitic manganese steel' *Proc of the Third International Conference on Fracture (Munich, FRG, 1973)* paper III–425

3 **Rice, R.C. and Stephens, R.I.** 'Overload effects on subcritical crack growth in austenitic manganese steel' *Progress in Flaw Growth and Fracture Testing STP 536* (American Society for Testing and Materials, 1973) pp 95–114

4 **Owen, W.S., Pelloux, R.M.N., Ritchie, R.O., Faral, M., Ohhashi, T. and Toplosky, J.** 'The cyclic energy absorption and low-cycle fatigue life to four candidate steels' *University of California at Berkeley Report No. UCB/EERC–79/09 Vol 3 Part A (1979) pp A1–A35*

5 **Rittel, D. and Roman, I.** 'Effects of yield strength and phosphorus content on the high cycle fatigue properties of cast austenitic manganese steels' *Fatigue Life Analysis and Prediction* (American Society for Metals, 1986) pp 109–116

6 **Rittel, D. and Roman, I.** 'Tensile deformation of coarse grained cast austenitic manganese steels' (1988) *Mater Sci Engng* (1989) in press

7 **Rittel, D. and Roman, I.** 'Tensile fracture of coarse grained cast austenitic manganese steels' *Met Trans* **19A** (September 1988) pp 2269–2277

8 **Raske, D.T. and Morrow, J. D.** 'Mechanics of materials in low cycle fatigue' *Manual on Low Cycle Fatigue STP 465* (American Society for Testing and Materials, 1969) pp 1–25

9 ASTM Standards 'Standard testing method for constant load-amplitude fatigue crack growth above 10^{-8} m/cycle' *Annual Book of ASTM Standards E647* (American Society for Testing and Materials, 1983) pp 710–713

10 **Hertzberg, R.W.,** *'Deformation and Fracture Mechanics of Engineering Materials'* (J. Wiley and Sons, 1976) pp 446–447

11 **Hatanaka, K. and Fujimutsu, T.,** 'The cyclic stress–strain response and strain-life behaviour of metallic materials' *Fatigue 84 Vol 1 (EMAS, 1984)* pp 93–103

12 **Gorlier, C., Amzallag, C., Rieux, P. and Driver, J.H.** 'The cyclic plastic behaviour of a 316 Steel at 20 to 600°C' *Fatigue 84 Vol 1 (EMAS, 1984)* pp 41–48

13 **Pelloux, R.M.** 'Influence of grain size on fatigue' in *Ultrafine-Grain Materials* (Syracuse University Press, USA, 1969) pp 231–243

14 **Roberts, W.N.,** 'Deformation twinning in Hadfield steels' *Trans TMS AIME* **230** (April 1964) pp 372–377

15 **Rittel, D., Roman, I. and Bercovier, M.** 'Cyclic plastic zone characterization and its relation to fatigue crack growth' *Proc of Fourth International Conference on Numerical Methods in Fracture Mechanics* (San-Antonio, 1987) pp 627–640

Authors

The authors are with the Materials Science Division, Graduate School of Applied Science and Technology, The Hebrew University, Jerusalem 91904, Israel.